



---

# FFI-RAPPORT

---

17/01317

## Automatic ship detection and confidence estimates

—

Tonje Nanette Arnesen Hannevik  
Richard B. Olsen



# **Automatic ship detection and confidence estimates**

Tonje Nanette Arnesen Hannevik and Richard B. Olsen

---

## Keywords

Syntetisk apertur-radar (SAR)

Statistikk

Skipsdeteksjon

Polarisasjon

Satellitter

## FFI-rapport

FFI-RAPPORT 17/01317

## Prosjektnummer

1441

## ISBN

P: 978-82-464-2988-5

E: 978-82-464-2989-2

## Approved by

Richard B. Olsen, *Research Manager*

Johnny Bardal, *Director*

---

---

## Summary

The Norwegian Defence Research Establishment (FFI) has been doing research on ship detection in Synthetic Aperture Radar (SAR) imagery since the late 1980's, and the Norwegian Armed Forces have used SAR images operationally since 1998. From the beginning and until now there has been a growing interest in operational ship detection. There are many key questions in operational ship detection, and one is confidence levels for ship detection. That question and other factors related to confidence levels are being looked at in this report.

One way of making confidence estimates is to gather evidence that can support a decision whether the vessel is a real ship or a false alarm. The ship size, ship-to-sea contrast, morphology and ship wake detection can be used as pieces of evidence. The incidence angle of the SAR satellite (e.g. if the satellite looks near-range or far-range) will affect the ability to detect a vessel at sea. In addition, the latest SAR satellites have the possibility to acquire more images each with different polarizations. Information about incidence angle and polarization can be used to improve the confidence estimate.

The algorithms described in this report can be improved over time with more validated data available. Land based and space based Automatic Identification System (AIS) data should be used to be able to provide significant input to the algorithms for validation of ship detection in SAR imagery.

FFI has developed an automatic ship detection tool, AEGIR, which detects vessels in all polarisation channels. The algorithms described are implemented in AEGIR.

---

---

## Sammendrag

Forsvarets forskningsinstitutt (FFI) har forsket på skipsdeteksjon i syntetisk apertur-radar-bilder (SAR) siden sent på 1980-tallet, og Forsvaret har brukt SAR-bilder operasjonelt siden 1998. I løpet av denne perioden har det vært økende interesse for operasjonell skipsdeteksjon. Det er mange nøkkeltemaer å ta hensyn til når en skal utføre operasjonell skipsdeteksjon, og et av temaene er konfidensestimater for skipsdeteksjon. Dette spørsmålet og andre spørsmål relatert til konfidensestimater blir sett på i denne rapporten.

En måte å finne konfidensestimater på er å samle bevis som kan støtte en i å avghøre om det virkelig er et skip som blir detektert, eller om det er falsk alarm. Skipsstørrelse, skip-til-sjø-kontrast, skipets form og kjølevannstriper kan brukes som bevis. Innfallsvinkelen til SAR-satellitten (om den ser bratt ned eller langt ut over sjøen) endrer deteksjonsevnen. I tillegg gir de nyeste SAR-satellittene muligheten for å få flere bilder med forskjellige polariseringer. Informasjon om innfallsvinkel og polarisering kan brukes til å forbedre konfidensestimater.

Algoritmene som er beskrevet i denne rapporten kan forbedres over tid med validerte data tilgjengelig. Landbaserte og rombaserte Automatic Identification System-data (AIS) bør brukes for å gi signifikant informasjon til algoritmene for å validere skipsdeteksjon i SAR-bilder.

FFI har utviklet en automatisk skipsdeteksjonsalgoritme, ÆGIR, som detekterer skip i alle polariseringskanaler. Algoritmene som er beskrevet i rapporten, er implementert i ÆGIR.

---

---

# Content

<b>Summary</b>	<b>3</b>
<b>Sammendrag</b>	<b>4</b>
<b>1 Introduction</b>	<b>7</b>
<b>2 Approach</b>	<b>7</b>
2.1 Wind estimates	8
2.2 Determination of wind direction	12
2.3 Radar cross section and ship size	13
2.4 Minimum detectable ship size	13
2.5 Ship to sea contrast	16
2.6 Morphology	16
2.7 Wake detection	17
<b>3 Algorithms</b>	<b>20</b>
3.1 Evidence gathering	20
3.2 Detection in multiple polarisation channels	22
3.3 Hypothesis testing	24
<b>4 Recommendations and conclusions</b>	<b>27</b>
<b>References</b>	<b>28</b>
<b>Abbreviations</b>	<b>29</b>





---

---

# 1 Introduction

FFI has worked with ship detection in SAR (Synthetic Aperture Radar) imagery from SEASAT, ERS-1, ERS-2, ENVISAT, RADARSAT-1 and RADARSAT-2 since the late 1980's. During this period there has been a world-wide growing interest in operational use of SAR imagery for ship detection. Some of the key questions in ship detection are:

1. Efficiency of different algorithms?
2. Which signatures should be used for detection?
3. False alarm rate?
4. Minimum detectable ship size?
5. Probability of detection (or probability of missing ships)?
6. Confidence levels for detection?
7. Which mode(s) is (are) most useful? (for radars from the late 1990's)

In this paper we take a look at question 6.

## 2 Approach

Confidence levels for detection of ships (or targets) are to some extent based on factors related to the questions above. For example, if the detector is set to provide a relatively high false alarm rate, we can be less confident about the probability of a candidate actually being a ship, unless we also can find some properties about the target that support the conclusion that the target candidate really is a ship. One of the most immediate "pieces of evidence" is the estimated size of the target. If the size approaches the minimum detectable ship size, then we must be less confident that the detected target really is a ship. Confidence estimates can be based on any or all of the following "pieces of evidence":

- Information about the environmental (METOC - Meteorology and Oceanography) conditions.
- A model for the relationship between METOC conditions, relevant SAR image parameters and minimum detectable vessel size.

- 
- 
- A model for the relationship between a vessel's Radar Cross Section (RCS) and the vessel size.
  - Ship-to-sea contrast.
  - Morphology of the detected candidate vessel.
  - Presence of a detected wake signature.
  - Statistics for the expected number of ships in the area of the SAR image.
  - Statistics for expected presence of other features (e.g. wake look-alikes).

For multi-channel data, AP (Alternating Polarisation) mode data from ENVISAT or polarimetric data from TerraSAR-X, COSMO SkyMed or RADARSAT-2):

- Has the candidate target been detected in more than one channel?
- What is the incidence angle for the detected target?

The evidence should be used to answer the following questions:

- Is the estimated size of the detected candidate large enough to be detected with the prevailing wind conditions and nominal radar parameters? If so, how much larger than the estimated minimum is it?
- Is there more than one piece of evidence that supports the supposition that a ship has been detected?
- Do we in fact expect to detect many ships in the imaged area?

An operational algorithm should have enough built in flexibility to deal with different scenarios, depending on the data at hand (SAR mode, calibrated products, external sources of information on METOC conditions and ship traffic levels etc). In the following, we outline the strategy to be used for some important factors.

## **2.1 Wind estimates**

Ocean backscatter (clutter) is dependent on wind conditions. Wind can be estimated from SAR data directly by several means. One of the most common is using the CMOD (C-band MODel) algorithm for VV- polarised (Vertical transmit-vertical receive) ocean backscatter, as is used for the ERS scatterometer data [1].

$$\sigma_0 = A + B \cos \varphi + C \cos 2\varphi \ ; \ A = a(\theta) U^{\gamma_a(\theta)}, \dots \quad (1)$$

where  $\varphi$  is the angle between the radar range direction and the wind direction. The coefficients  $A$ ,  $B$  and  $C$  depend on the wind speed and incidence angle, as well as radar frequency and polarisation. Figures 2.1 – 2.4 show various depictions of the CMOD function. Figure 2.5 shows an example of a SAR image with wind-induced streaks.

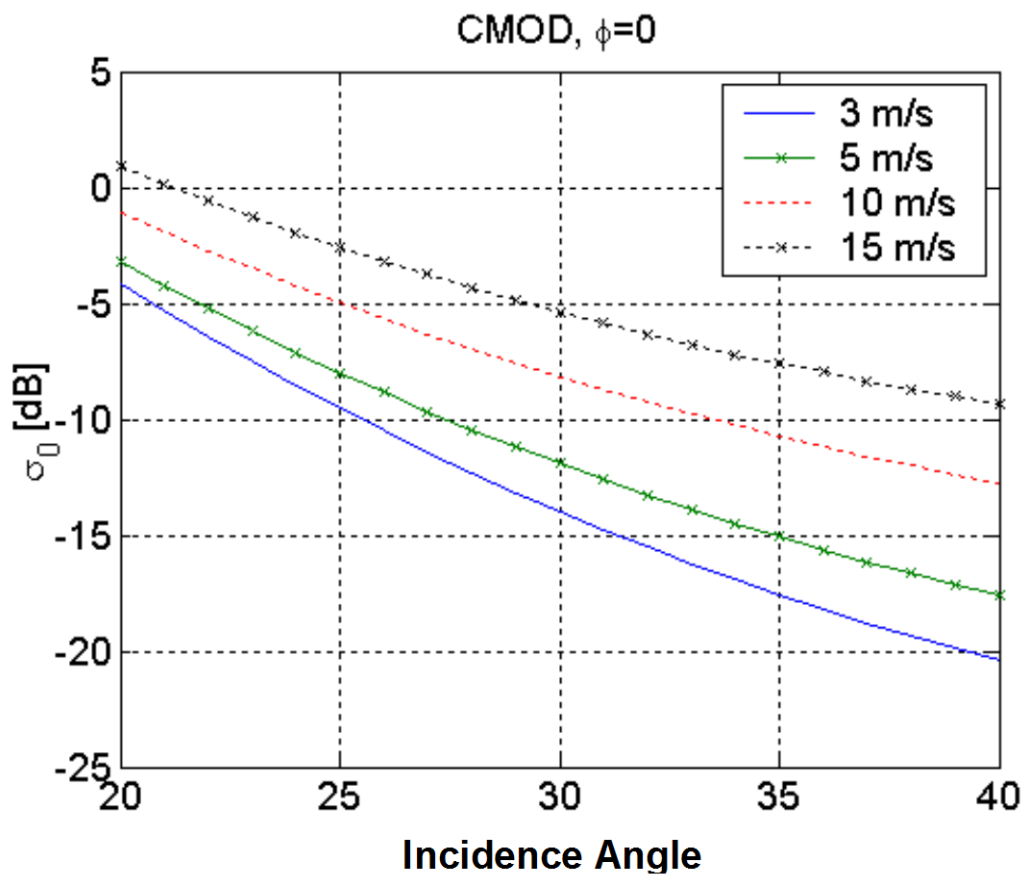


Figure 2.1 Normalized radar cross-section as a function of incidence angle, for different wind speeds, calculated using CMOD (C-band, VV-polarisation, with the radar looking upwind).

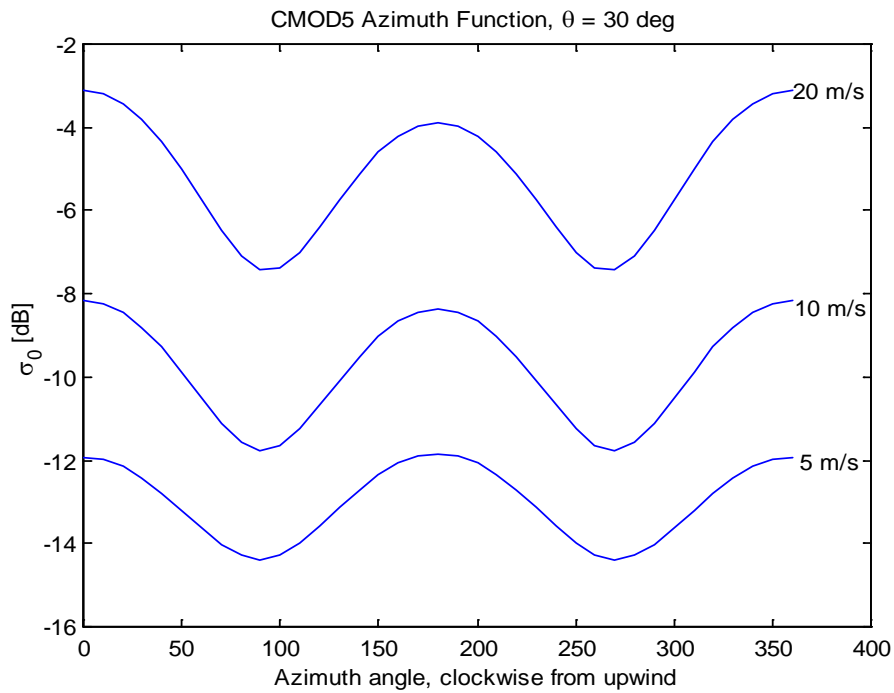


Figure 2.2 Normalised radar cross section at an incidence angle of  $30^\circ$ , as a function of angle between the range direction and the wind direction, calculated using CMOD.

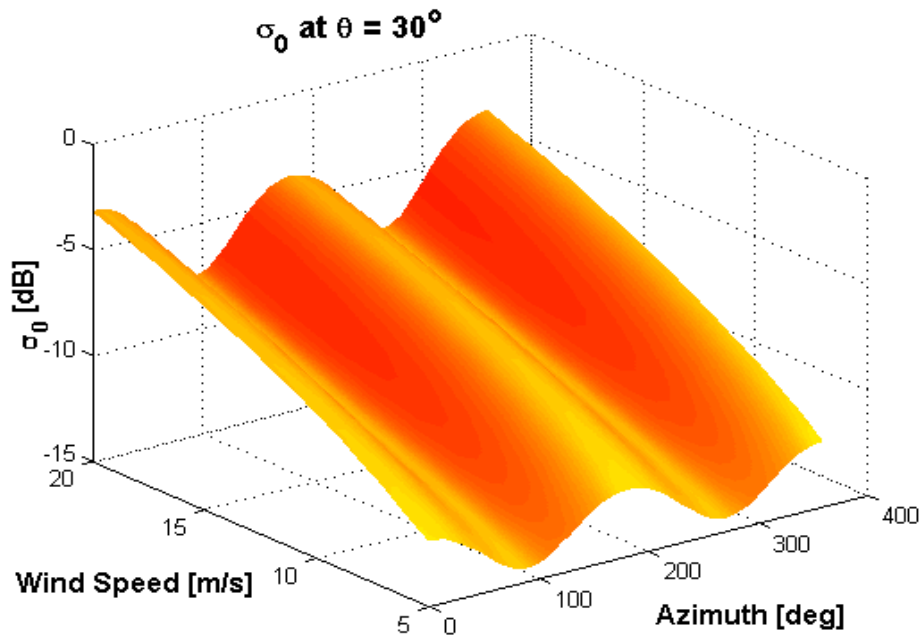


Figure 2.3 Radar backscatter from the ocean surface as a function of wind speed and azimuth angle ( $\varphi$ ) for an incidence angle of  $30^\circ$ .

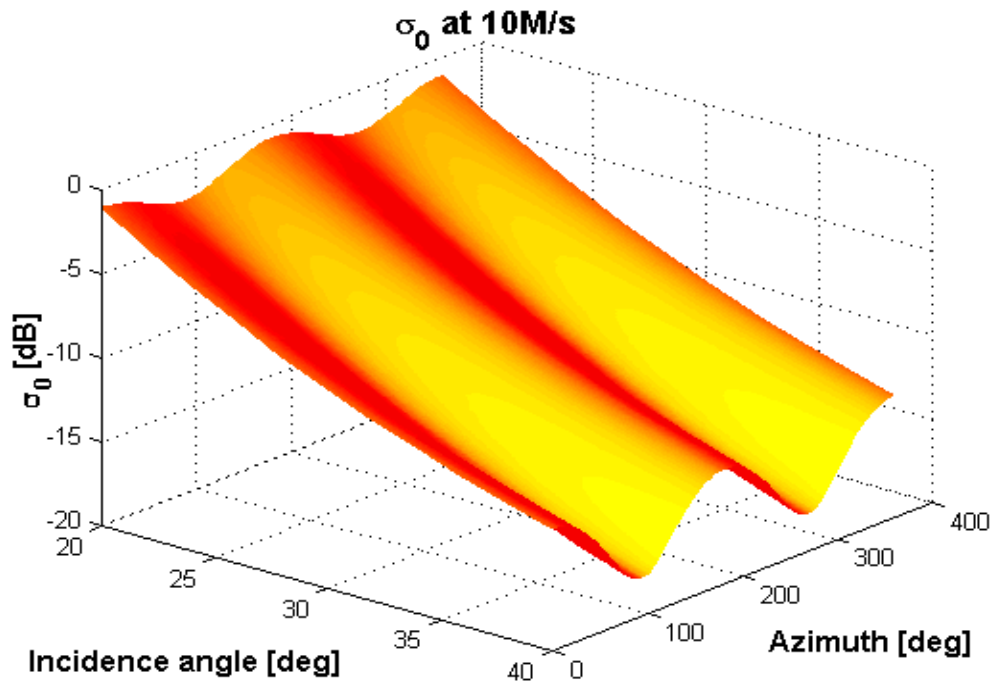


Figure 2.4 Radar backscatter from the ocean surface as a function of incidence angle and azimuth angle  $\varphi$  for a wind speed of 10 m/s.

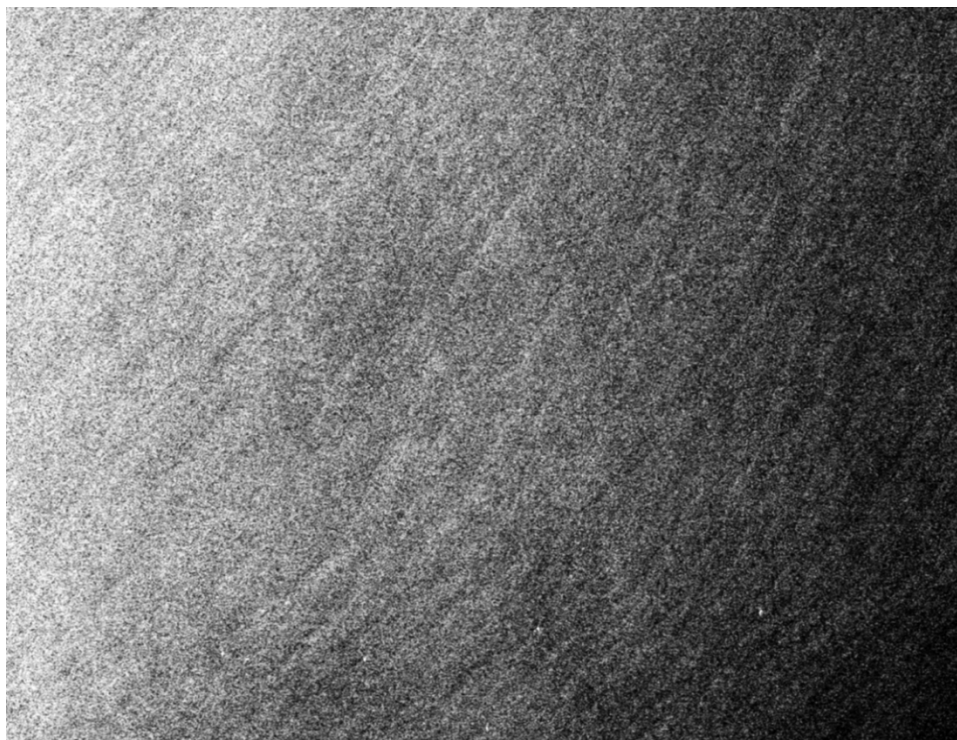


Figure 2.5 Example of SAR image with wind-induced streaks.

---

Some basic requirements for using the CMOD approach are:

- Calibrated data
- Suitable conditions for determining wind direction
- A suitable conversion model for application to HH-polarisation and cross-polarisation data.

If these requirements are not met, an alternate source needs to be supplied:

- Other sensor data
- Atmospheric model data
- Weather charts

This could be scatterometer data, in situ observations, output from atmospheric forecast models (e.g. GRIB files) or an estimate read off a weather chart.

## 2.2 Determination of wind direction

Several publications have shown how to determine wind direction from patterns in a SAR image. Most of them start with the two-dimensional Fourier transform of a piece of an image, as shown in Figure 2.6. Efforts have been made to fit model surfaces, such as Gaussians, to the data, with varying degrees of success. If the chosen surface function is a poor match for the data, the results tend to be unpredictable. Another approach that seems to work quite well is based on principal components, also known as Empirical Orthogonal Functions (EOFs), which is described in section 2.6.

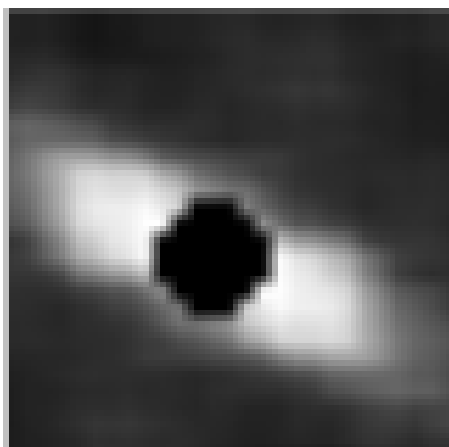


*Figure 2.6 Example of a two-dimensional Fourier transform from the SAR image in Figure 2.5. The centre is shown in detail in the in-set.*

---

---

### 2.3 Radar cross section and ship size

Skolnik [2] has published a simple empirical expression for estimating vessel size as a function of radar cross section:

$$\sigma_{ship} = D \quad (2)$$

where  $D$  is the ship displacement in metric tons. This relationship does not take into account radar parameters or imaging geometry. Skolnik has also suggested, however, that the radar cross section should decrease when observed at steeper incidence angles (for co-polarisation).

A more convenient parameter for estimating vessel size is vessel length (length at the waterline). Vachon et al [3] performed an analysis of length vs. displacement, and arrived at the following relationship:

$$\sigma_{ship} = D = 0.08048 \cdot l^{2.31} \approx 0.08 \cdot l^{7/3} \quad (3)$$

where  $l$  is the length in meters.

It is worth mentioning here that Skolnik's formula is developed without evaluating the load of a vessel. A vessel that is fully loaded displaces a larger amount of water than an empty one. Being fully loaded, however, it will have less exposure above the water, and can be expected to have a lower radar cross section. Vachon et al defined the displacement as that of a vessel fully loaded.

Vachon et al furthermore examined the incidence angle dependency, for angles between  $15^\circ$  and  $45^\circ$ , and arrived at the relationship:

$$R(\theta) = 0.78 + 0.11\theta \quad (4)$$

where  $R$  is the ratio of observed to expected radar cross section. Thus, we have the following expression, referred to as Vachon's formula below, for the relationship between a ship's radar cross section and its length:

$$l = \left( \frac{\sigma_{ship}}{0.08 \cdot R} \right)^{3/7} \quad (5)$$

### 2.4 Minimum detectable ship size

Using the expression in the previous section, various approaches may be taken to estimate the minimum detectable ship size, depending on the thresholding method that is used. A couple of options follow below.

---

**Rule of thumb:** Experience shows that in order to detect a ship, it should have a normalized radar cross section at least 10 dB above the ocean background clutter. Using the expression

$$\sigma_{ship}^{min} = \rho_r \rho_a 10^{(\sigma_{sea} + T)/10} \quad (6)$$

and  $T=10$  dB, we can obtain an estimated minimum detectable ship length, using Vachon's formula.

**CFAR approach:** Ocean clutter has been demonstrated to follow a K-distribution [4], given by:

$$p_I(I) = \frac{2}{\Gamma(N)\Gamma(\nu)} \left(\frac{N\nu}{\mu_I}\right)^{\frac{N+\nu}{2}} I^{\frac{N+\nu-2}{2}} K_{\nu-N} \left[ 2\sqrt{\frac{\nu NI}{\mu_I}} \right] \quad (7)$$

where  $N$  is the effective number of looks,  $I$  is the image intensity,  $\mu_I$  is the average image intensity,  $\Gamma$  is the gamma function and  $K$  is the modified Bessel function of order  $\nu-N$ .  $\nu$  is an order parameter that needs to be determined from a fit to the data. Figure 2.7 shows some examples of the K-distribution for typical values of  $\nu$ .

In order to find a threshold  $I_T$  with a given false alarm rate  $\eta_T$ , the K-distribution function has to be integrated:

$$\eta_T = \int_0^{I_T} p(x) dx \quad (8)$$

For a given threshold intensity level,  $I_T$ , and an average intensity value of unity, the minimum detectable vessel cross section is given by:

$$\sigma_{ship}^{min} = I_T \sigma_0 \rho_a \rho_r \quad (9)$$

where  $\sigma_0$  is the ocean's normalised radar backscatter, and  $\rho_a$  and  $\rho_r$  are the radar azimuth and range resolutions. The minimum vessel size is therefore heavily dependent on the ocean backscatter,  $\sigma_0$ , which varies with radar viewing geometry, polarisation, frequency, wind speed and wind direction relative to the radar look direction.

Figure 2.8 shows estimates of minimum detectable ship size using the CFAR (Constant False Alarm) approach, and assuming that the radar is looking into the wind. As the results are purely an estimate, the resulting quantity is often referred to as a Figure of Merit (FOM).



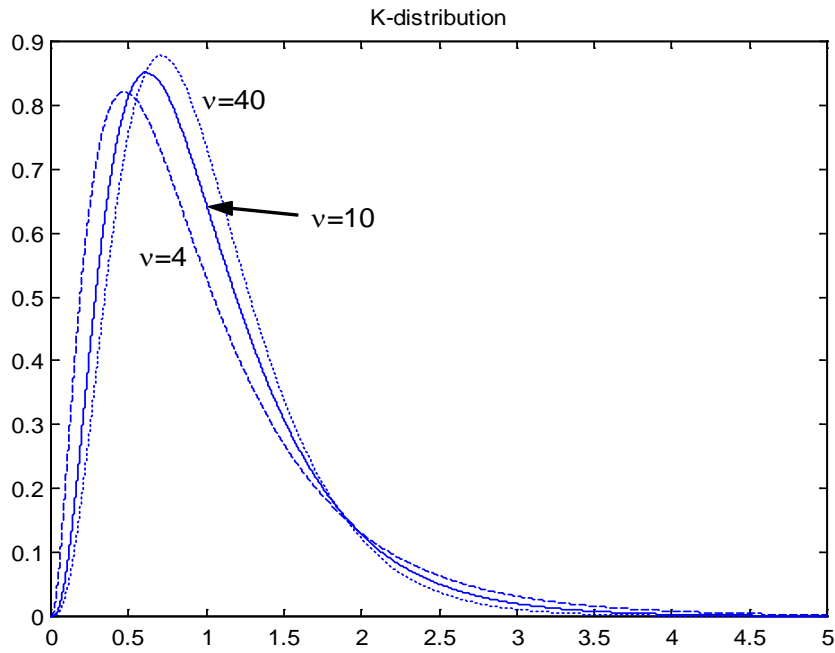


Figure 2.7 K-distribution for different values of the order parameter  $\nu$ .

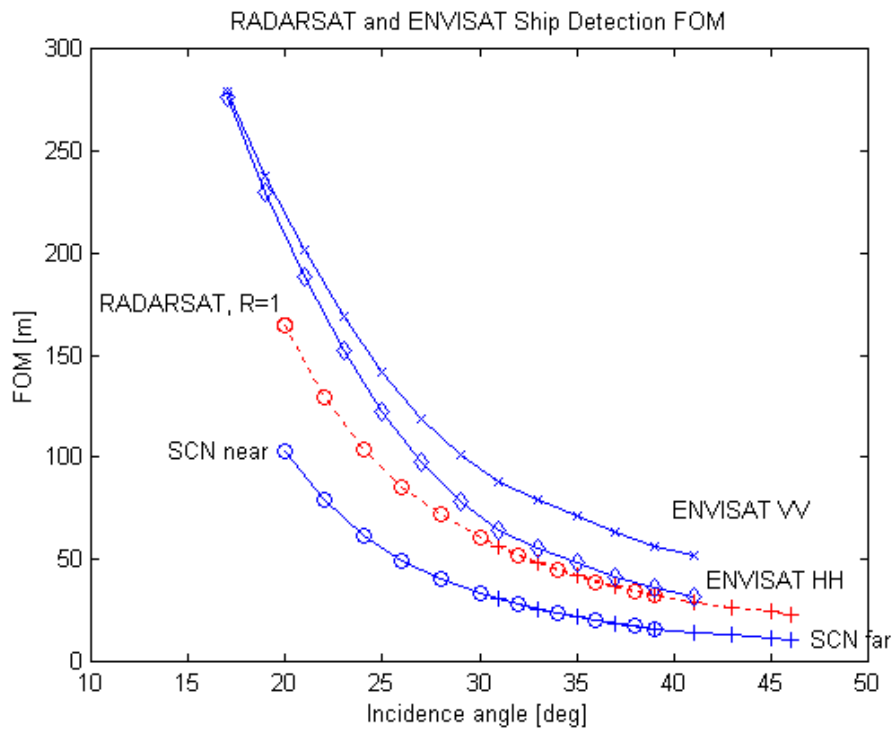


Figure 2.8 Estimate of minimum detectable ship size for 10 m/s wind, radar looking up-wind. The estimate is a Figure of Merit, and is indicative of the sizes that could be detectable.

---



---

## 2.5 Ship to sea contrast

The ship to sea contrast can be estimated using the expressions:

$$\sigma_0^{ship} = 10 \log \left| \frac{\sigma_{ship}}{\rho_a \rho_r} \right| \quad [dB] \quad (10)$$

$$Contrast = \sigma_0^{ship} - \sigma_0^{sea}$$

## 2.6 Morphology

Ship target pixels form a more or less elliptical cluster (see Figure 2.9). A robust approach to analysing the cluster dimensions is the method of Empirical Orthogonal Function analysis (EOFs), also known as principal component analysis.

An EOF analysis is used to derive a set of orthogonal functions that in total describe the data set under-going analysis. Instead of using analytic orthogonal functions, e.g. Fourier or Laplace, the EOFs are derived from the data itself. For an N-dimensional data set, determining EOFs corresponds to a coordinate transformation that rotates the coordinate system, such that the first coordinate describes the maximum possible fraction of the total variance in the data. It turns out that the way this is obtained is by determining the variance/co-variance matrix for the data, and using its eigenvectors as the vector basis for the new coordinate system. Specifically for a two-dimensional data set,  $D$ , we have a variance/co-variance matrix:

$$\mathbf{C} = \begin{bmatrix} S_{xx} & S_{xy} \\ S_{xy} & S_{yy} \end{bmatrix} \quad (11)$$

where:

$$S_{xx} = \frac{1}{(\Delta x)^2} \sum_{i=1}^N \sum_{j=1}^M x_j^2 D_{ij}$$

$$S_{yy} = \frac{1}{(\Delta y)^2} \sum_{i=1}^N \sum_{j=1}^M y_i^2 D_{ij} \quad (12)$$

$$S_{xy} = \frac{1}{\Delta x \Delta y} \sum_{i=1}^N \sum_{j=1}^M x_j y_i D_{ij}$$

The eigenvectors for this matrix will be orthogonal, and can be used to define a new coordinate system with a new x-axis parallel with the first eigenvector and a new y-axis parallel with the second eigenvector.

Applying equations (11) and (12) to the pixels exceeding the detection threshold, we obtain a length and width estimate based on the absolute values of the eigenvectors of the variance-covariance matrix of an image chip centred on the ship.

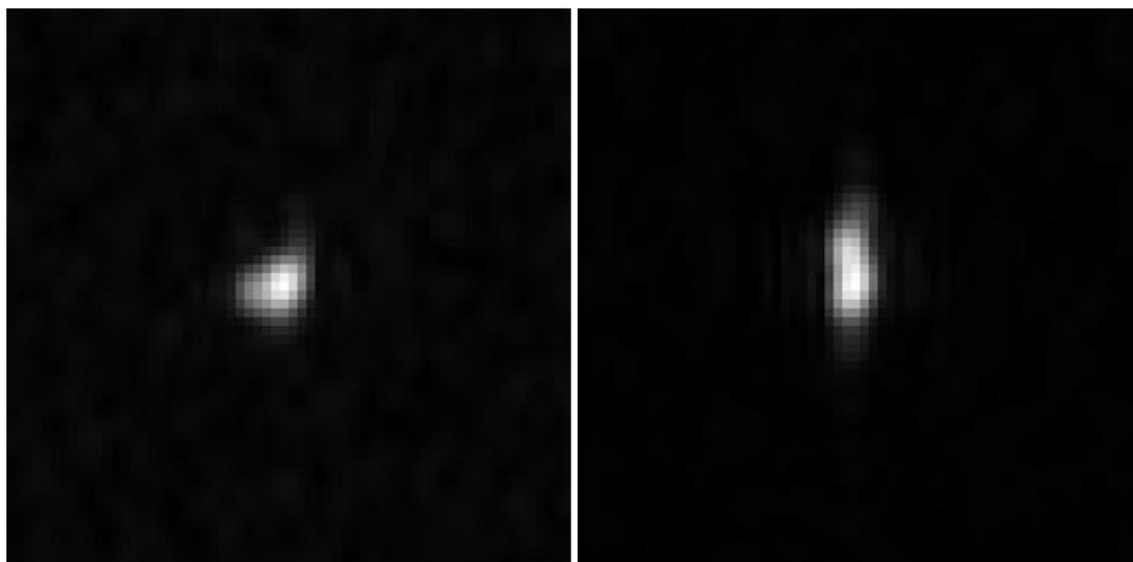


Figure 2.9 Example of ships in SAR images

## 2.7 Wake detection

Figure 2.10 shows typical wave patterns around a ship under way, while Figure 2.11 shows an example of observed ship wakes in an ERS-1 SAR image.

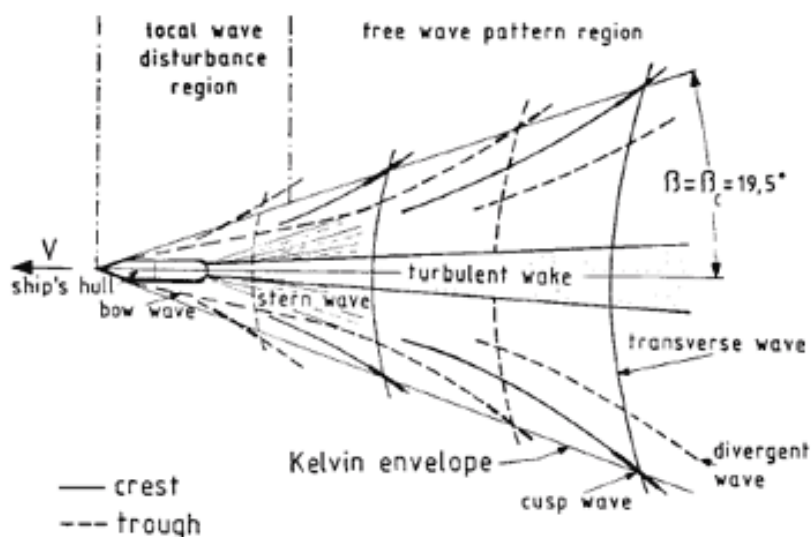
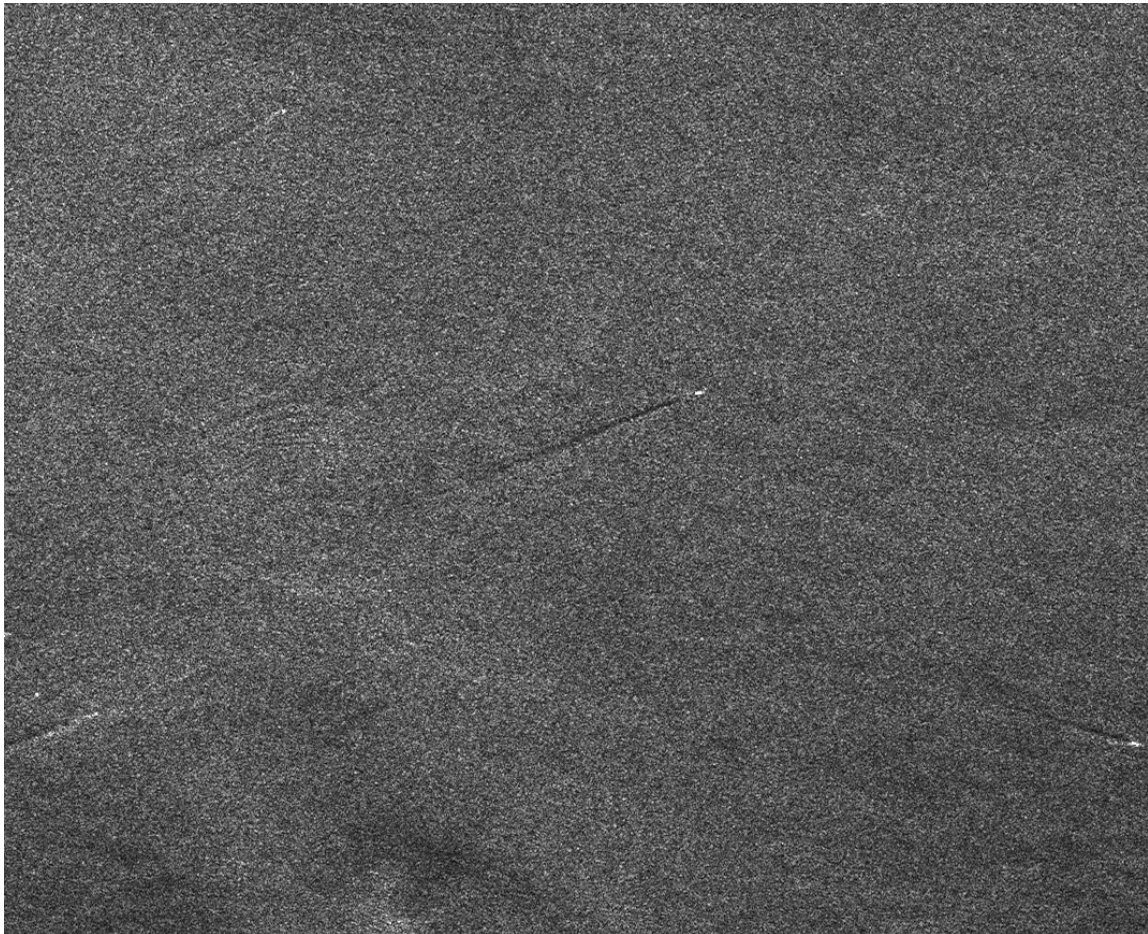


Figure 2.10 Typical ship wakes causing signatures in SAR imagery [5].



*Figure 2.11 Example of ships and ship wakes in an ERS-1 SAR image.*

Wave patterns generated by ships are set up at both the bow and the stern. These waves interact with each other and with other waves on the ocean surface, and the results may be observed in several ways in SAR images. In addition, ships leave behind a band of turbulence that may persist for hours. The turbulent motion interacts with surface waves, and is often observed in SAR images as a dark streak, referred to as a dark turbulent wake.

Ship wakes in light wind and calm sea conditions often appear as a bright V-shape with a half-angle of 2-3 degrees. The Bragg scattering mechanism has been used as a basis to explain this phenomenon. It is believed that the narrow V-wake is not a part of the Kelvin wake itself. Alternatively, it has been suggested [6] that short divergent Kelvin waves may contribute to the V-wake, even though the waves are mixed with unsteady surface waves, which are generated by ship-induced turbulence. In some cases the ocean surface conditions result in the Bragg waves being blocked. This in turn results in a corresponding dark wake signature in an image.

In very high resolution imagery, typically airborne SAR, the transverse waves from the stern of a ship can be seen. These waves travel at the speed of the ship, and their wavelength can be used to estimate the ship's speed, using the expression:

$$c_p = \sqrt{\frac{g\lambda}{2\pi}} \quad (13)$$

where  $c_p$  is the phase velocity of the waves (and hence the ship's velocity), and  $\lambda$  is the wave length.

Various methods have been investigated for detection of wakes in SAR imagery. In [7], a wake search around the detected ships is done along a line in the azimuth direction, drawn through the vessel candidate. For each position along this line, a set of scan lines sampled at fixed angular intervals, are used to extract profiles of pixel values. Each profile is averaged to one value, and then a scan curve emerges, which consists of relative intensity as a function of angle around the search point. A polynomial fit is done to the curve to produce a smoothed curve, which is offset several deviations to form upper and lower thresholds (see Figure 2.12). Peaks and valleys are then examined further to filter out possible ships and ship wakes, by using least square method together with Chebyshev polynomials up to a certain order.

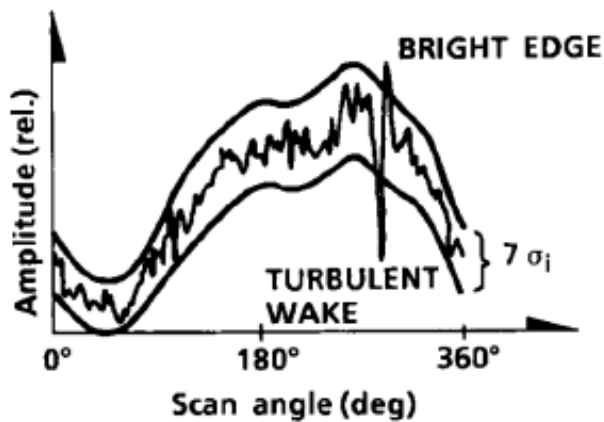


Figure 2.12 Example of wake scan curve from [7].

An alternative approach involves using the Radon transform for automatic ship wake detection. The Radon transform is given in the continuous domain by:

$$f(r, \nu) = \iint_A p(x, y) \delta(r - x \cos \nu - y \sin \nu) \quad (14)$$

where  $A$  is the image plane,  $p(x, y)$  is the pixel value at position  $(x, y)$ ,  $r$  and  $\nu$  are the range and orientation coordinates of a straight line, and  $\delta$  is the Dirac delta function. The Radon transform

---

---

results in a surface with strong maxima and minima for significant bright and dark lines, and can therefore be exploited in an automatic detector.

### 3 Algorithms

As mentioned in the introduction, an approach to confidence estimates (CE) may be based on gathering evidence to support decisions on whether or not a detected candidate vessel is a real ship or a false alarm. Pieces of evidence can be given weighting factors depending on availability and reliability. In the following sections we discuss evidence gathering and hypothesis testing.

#### 3.1 Evidence gathering

Taking the evidence gathering approach, we look at:

Ship Size	(A)
Ship to Sea Contrast	(B)
Morphology	( $\Gamma$ )
Wakes	( $\Delta$ )

to estimate a Figure of Merit for confidence:

$$CE = \frac{aA + bB + c\Gamma + d\Delta}{a + b + c + d} \quad (15)$$

The weighting factors need to be determined on the basis of test data sets. The factors can be defined based on how much the user want to emphasize each of ship size, ship to sea contrast, morphology and wakes. With RADARSAT-2 where few wakes are observed, this factor can be set to zero. Details of the remaining calculations follow below.

These points are used to find the ship size:

- Estimate ship size using Vachon's formula
- Set max expected ship size based on statistics for historical ship sizes in the area north of Bergen if the interest areas are the areas in the High North.
- Estimate minimum expected detectable ship size for each mode for the satellites available.

An appropriate expression for ship size evidence is:

$$A = \frac{l_{\text{obs}} - l_{\text{min}}}{l_{\text{max}} - l_{\text{min}}} \quad (16)$$

$l_{\text{obs}}$  is the length estimated using Vachon's formula.  $l_{\text{min}}$  and  $l_{\text{max}}$  are defined by the user before the ship detection is done. Figure 3.1 shows the distribution of vessels sizes of 2673 vessels during 6 months in Norwegian Sea and Barents Sea north of 71°N. The figure shows that there were no vessels above 350 m inside the area during half a year.

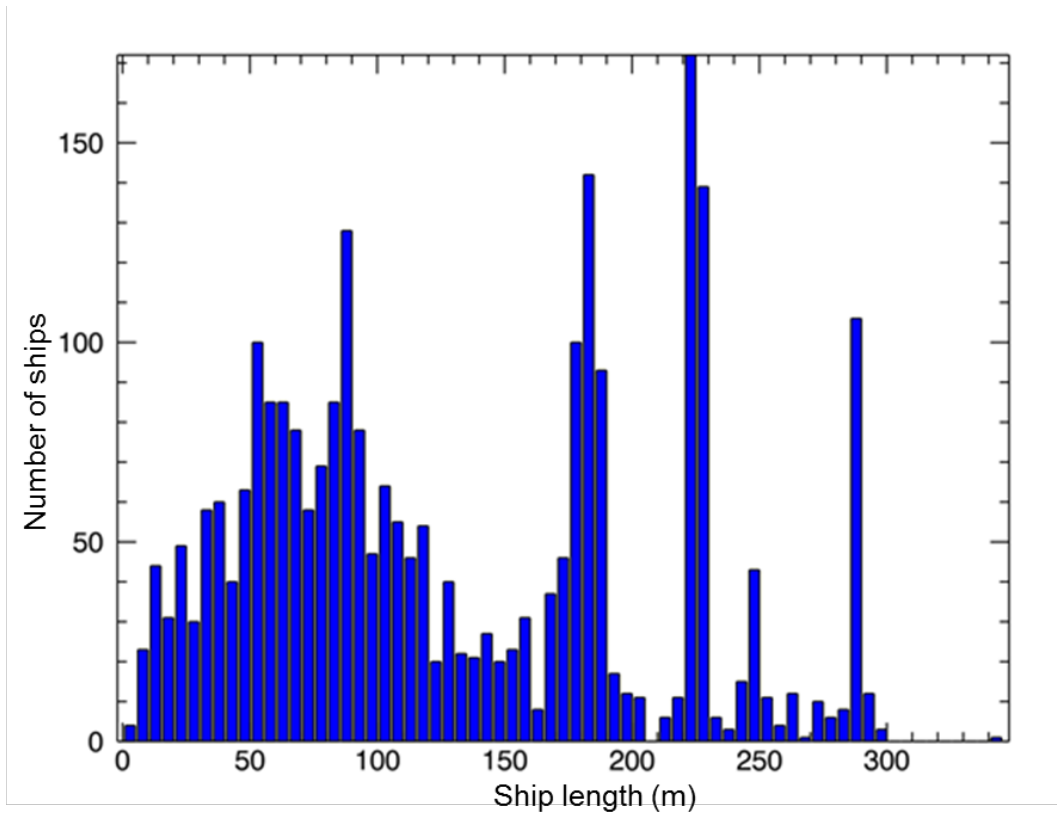


Figure 3.1 Distribution of vessel sizes in the Northern areas north of 71°N (Reference: AISSat-1 data, FFI).

**Ship to sea contrast:**

The following ship to sea contrast empirical gain function is proposed based on a method presented in [8]:

$$B = 1 + 0.5 \tanh(\beta(\text{contrast} - \gamma)) \quad (17)$$

**Morphology:**

The width and length are estimated using the method described in Section 2.6. The Morphology measure can be calculated straight forward using:

---



---


$$\Gamma = \frac{width}{length} \quad (18)$$

If the vessels ratio is within a certain border, then it will be weighted higher.

**Wake detection:**

Here, we propose to use a simple approach based on the number of identifiable wake arms:

$$\Delta = n_{wakes} / 3 \quad (19)$$

assuming that one is able to detect either a dark turbulent wake and/or one or two narrow V-shaped wake arms.

Experience shows that operational users need the information broken down in the simplest terms possible. The confidence measures are therefore also reported in a simple manner, on a scale of 0-3, where a 3 indicates certain ship detection (or as certain as one can possibly be).

**3.2 Detection in multiple polarisation channels**

Confidence estimates are added to the ship detection reports for all detections for each polarisation channel. The number for Figure of Merit for confidence, that is found using the method described in section 3.1, is used as a basis. In addition the following algorithm described in this section is used to change the confidence estimate depending on if the vessel is detected in one or more polarisation channels and depending on which incidence angel the detection is done.

The detection of vessels against a sea background is dependent of several factors, for example incidence angle, polarisation, wind and sea state, ship’s direction compared to radar, ship’s superstructure, the radar frequency and more. Originally, when detection was done with RADARSAT-1 that offered HH-polarisation (Horizontal transmit-Horizontal receive), high incidence angles were needed to do ship detection in co-polarisation. When ENVISAT, RADARSAT-2, TerraSAR-X, and the COSMO SkyMed satellites were available, research on these satellites have shown that cross-polarisation (HV (Horizontal transmit-Vertical receive) and VH (Vertical transmit-Horizontal receive)) can be used for ship detection for smaller incidence angles. For incidence angles above approximately 35 degrees both co- and cross-polarisation channels can be used to do ship detection [9]. All this information is important when implementing an algorithm where incidence angle and detections in one or more polarisation channels shall be taken into account.

For dual-polarisation the algorithm in Table 3.1 to tune the confidence estimate is proposed. By detection in one channel 20 or 40 are added or subtracted depending on 1) the incidence angle ( $\theta$ ) and 2) if the probability is high or low to detect a target in the other polarisation channel.



Table 3.1 Algorithm to change/tune confidence estimate for dual-polarisation.

Polarisation combination	$\theta$ below $35^\circ$		$\theta$ above $35^\circ$	
	Detection in	CE change	Detection in	CE change
HH/HV	HH & HV	+ 60 HH + 60 HV	HH & HV	+ 60 HH + 60 HV
	HV	+ 40 HV	HH or HV	+ 20 HH + 20 HV
VV/VH	VV & VH	+ 60 VV + 60 VH	VV & VH	+ 60 VV + 60 VH
	VH	+ 40 VH	VH	+ 20 VH
	VV	- 40 VV	VV	- 20 VV
HH/VV	HH & VV	+ 40 HH + 40 VV	HH & VV	+ 60 HH + 60 VV
	HH	+ 20 HH	HH	+ 20 HH
	VV	- 20 VV	VV	- 20 VV

For VV/VH the following point is taken into account:

- The probability is low to detect a vessel in VV and not in VH for all incidence angles

For HH/VV the following points are taken into account:

- The probability is low that there will be a detection in VV and not in HH for all  $\theta$ .
- The probability is low to detect a vessel in VV:
- If there is a detection for small  $\theta$  in VV, but not in HH, 40 is subtracted from the confidence estimate
- If there is a detection for high  $\theta$  in VV, but not in HH, 20 is subtracted from the confidence estimate
- It is more probable that a vessel will be detected for high  $\theta$  in VV than for low  $\theta$ .

For quad-polarised data the algorithm in Table 3.2 to tune the confidence estimate is proposed. If the detection of a vessel is done under  $35^\circ$  in HH and VV, but not in the cross-polarisation channels, it is probable that the detection is false. Thus, 20 is subtracted from the confidence estimate

Table 3.2 Algorithm to change/tune confidence estimates for quad-polarisation data.

$\theta$ below $35^\circ$		$\theta$ above $35^\circ$	
Detection in	CE change	Detection in	CE change
HH	- 20 in HH	HH	+ 20 in HH
VV	- 20 in VV	VV	- 10 in VV
HV or VH	+ 20 in HV or VH	HV or VH	0
HV & VH	+ 40 in HV & VH	HV & VH	+ 20 in HV & VH
HH & HV or HH & VH	+ 40 in HH & HV or + 40 in HH & VH	HH & HV or HH & VH	+ 40 in HH & HV or + 40 in HH & VH
VV & VH or VV & HV	0	VV & VH or VV & HV	+ 10 in HH & HV or + 10 in HH & VH
HH & VV	0	HH & VV	+ 40 in HH & VV
3 channels	+ 40 in 3 channels	3 channels	+ 40 in 3 channels
4 channels	+ 60 in all channels	4 channels	+ 60 in all channels

### 3.3 Hypothesis testing

An alternative, and maybe somewhat more stringent, approach is to use hypothesis testing as discussed in [8], where the Dempster-Shafer method is applied to analyse ship wakes in an automatic detector.

The Dempster-Shafer method was developed as an approach to combine evidence from several sources (sensors). “Estimates of belief” are applied to decisions about the truth of a hypothesis. Peaks detected by a Wiener filter belong to one of the following hypotheses:

1. There exists a linear feature which belongs to a ship wake.
2. There exists a linear feature which does not belong to a ship wake.

A third possible conclusion is uncertainty of which of the two hypotheses the peak belongs to. The probabilities for the three possible conclusions, based on analysis of the Wiener filter output, are labelled  $pd_1$ ,  $pd_2$ , and  $pd_3$ . Evidence from a second sensor gives new probabilities and uncertainty  $p_1$ ,  $p_2$ , and  $p_3$ . An evidence “mass” is computed for each possible conclusion by the Dempster-Shafer rule of combination, as given in Table 3.3 where  $k$  is used to identify contradictory hypotheses.

Table 3.3 Dempster-Shafer rule of combination.

	pd1	pd2	pd3
p1	p1pd1	k	p1pd3
p2	k	p2pd2	p2pd3
p3	p3pd1	p3pd2	p3pd3

The masses of the three hypotheses are given by:

$$\begin{aligned}
 m_1 &= p1pd1 + p1pd3 + p3pd1 \text{ (wake feature)} \\
 m_2 &= p2pd2 + p2pd3 + p3pd2 \text{ (natural feature)} \\
 m_3 &= p3pd3 \text{ (uncertainty)}
 \end{aligned}
 \tag{20}$$

The masses are normalized and new updated probability values are obtained for the hypotheses.

A similar approach could be used for analysis of target detections:

- Hypothesis 1: Target is a ship
- Hypothesis 2: Target is a natural feature or noise

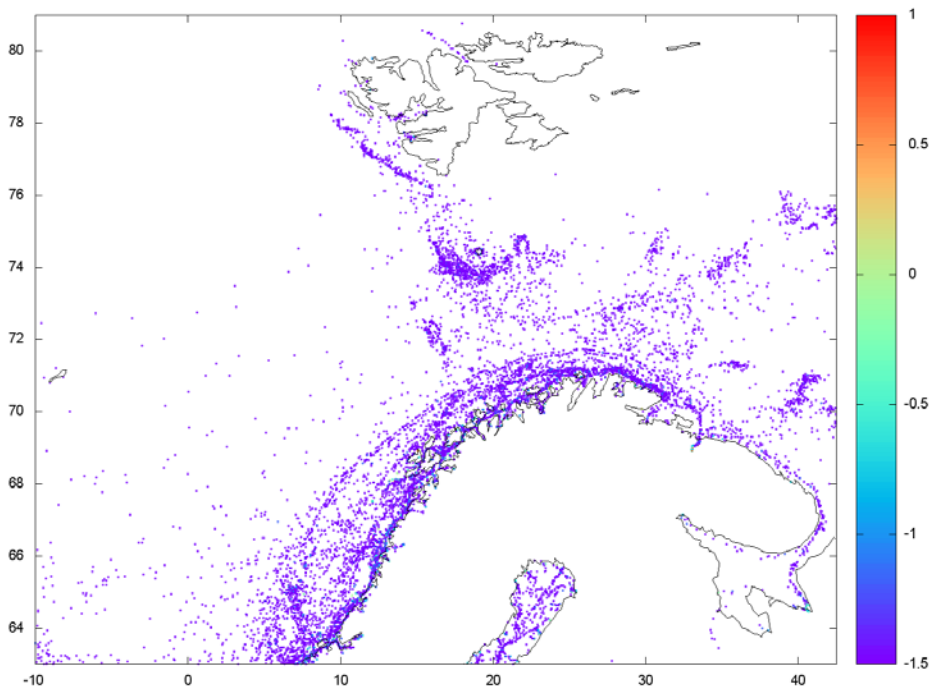


Figure 3.2 Typical distribution of vessel positions based on data from AISSat-1 during one month (Source: AISSat-1 data, FFI)

---

The probabilities could be based on target size and ship to sea contrast ratios. Evidence from the wake analysis and target analysis could furthermore be combined in a final Dempster-Shafer combination to arrive at a final confidence estimate.

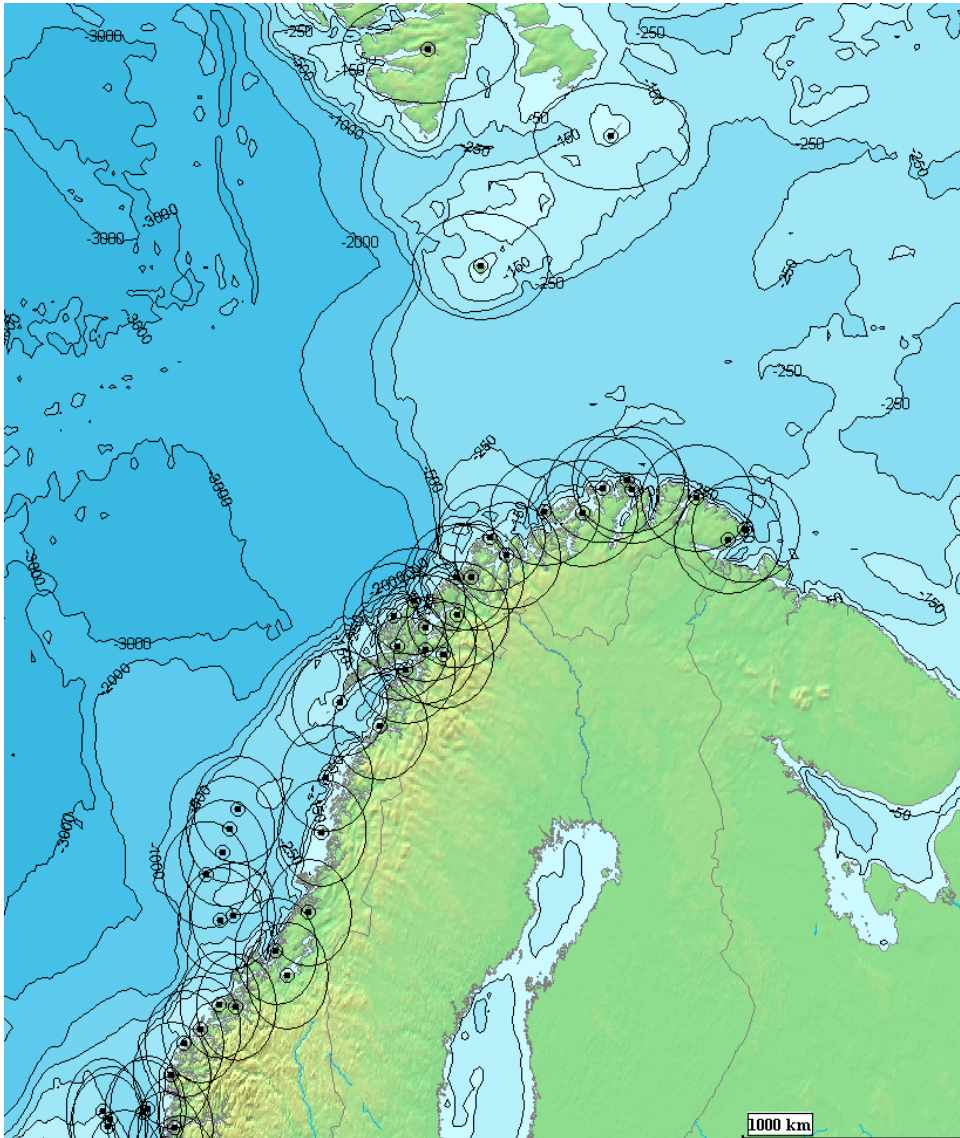


Figure 3.3 Coastal AIS stations and their coverage (© aisonline.com).

A key question again is how does one establish the weight factors in the belief functions? These could be based on existing statistics for ship traffic. The Automated Identification System governed by the International Maritime Organization is also a potentially valid source of ship data in coastal areas for land based AIS. In the open ocean, AISSat-1 and other AIS satellites can be used to get a picture. Figure 3.2 shows an example of a distribution of vessels based on data from AISSat-1 during May 2012. The figure shows how many vessels that are expected to be seen inside a given square if a random snapshot of the ship traffic is taken once during the month. Each side of the square is a minute of arc. The scale on the side is logarithmic. Sending

---

---

AIS signals is mandatory for all ships over 300 gross tons. The Norwegian Coastal Administration has installed a chain of AIS receiving stations for traffic monitoring in coastal waters (see Figure 3.3). AIS messages include information on ship size, heading, speed etc, which could be very useful information for validating ship and wake detection in SAR imagery.

## **4 Recommendations and conclusions**

The Norwegian Defence has used SAR images operationally since 1998, and an automatic ship detection tool will ease the tasks of analysing the SAR images. One important factor when doing automatic ship detection is to find confidence levels, which can help to decide whether the reported detection is a vessel or a false alarm.

One way of making confidence estimates is to gather evidence to support a decision whether the vessel really is a vessel or if it is noise or something else. Pieces of evidence that can be used are ship size, ship to sea contrast, morphology and ship wake detection. For SAR imagery where multiple polarisation channels are available, the estimated confidence estimate can be tuned depending on if the target is detected in one or more polarisation channels. The incidence angle also plays an important role for the decision if the target is a vessel or a false alarm. The algorithms described in this report are implemented in the automatic ship detection tool AEGIR. Based on the number of polarisation channels available and the incidence angle the vessel is detected at, the confidence estimate is tuned to give a better estimate.

The algorithms to estimate confidence estimates can be improved over time with more validated data available. AIS is available both from the coastal AIS chain and from satellite AIS. AIS data should be used continuously to be able to provide significant input to the algorithms for validation of ship detection in SAR imagery. This can be done in a future project.

---

---

## References

- [1] A. Stoffelen and D. L. T. Anderson, "ERS-1 Scatterometer Data Characteristics and Wind Retrieval Skill," ESA Special Publication SP-359, pp. 41-47, 1993.
- [2] M. I. Skolnik, Introduction to Radar Systems. New York, N.Y., USA: McGraw-Hill Book Company, 1982.
- [3] P. W. Vachon, J. W. M. Campbell, C. A. Bjerkelund, F. W. Dobson, and M. T. Rey, "Ship Detection by the RADARSAT SAR: Validation of Detection Model Predictions," Canadian Journal of Remote Sensing, vol. 23, no. 1, pp. 48-59, 1997.
- [4] C.J. Oliver, "Optimum Texture Estimators for SAR Clutter", J. Physics D:, vol. 26, issue. 11, pp. 1824-1835, 1993.
- [5] C. Melsheimer, H. Lim, and C. Shen, "Observation and Analysis of Ship Wakes in ERS-SAR and Spot Images", Asian Conference on Remote Sensing 1999.
- [6] G. Zilman and T. Miloh, "Kelvin and V-like Ship Wakes Affected by Surfactants," Journal of Ship Research 45, vol. 2, pp. 150-163, 2001.
- [7] K. Eldhuset, "An Automatic Ship and Ship Wake Detection System for Spaceborne SAR Images in Coastal Regions," International Journal of Remote Sensing, vol. 34, no. 4, pp. 1010-1019, 1996.
- [8] M. Rey, J. K. E. Tunaley, and T. Sibbald, "Use of the Dempster-Shafer Algorithm for the Detection of SAR Ship Wakes," IEEE Transactions on Geoscience and Remote Sensing, vol. 31, no. 5 1993.
- [9] T. N. A. Hannevik, "Evaluation of Radarsat-2 for ship detection," Forsvarets Forskningsinstitut,FFI-rapport 2011/01692, Dec.2011

---

---

## Abbreviations

AIS	Automatic Identification System
AP	Alternating Polarisation
CE	Confidence Estimate
CFAR	Constant False Alarm Rate
CMOD	C-band MODel
EOF	Empirical Orthogonal Functions
FFI	Forsvarets Forskningsinstitut
FOM	Figure Of Merit
H	Horisontal polarisation
HH	Horisontally transmitted – Horisontally received polarisation
HV	Horisontally transmitted – Vertically received polarisation
METOC	METeorology and OCEanography
RCS	Radar Cross Section
SAR	Synthetic Aperture Radar
V	Vertical polarisation
VH	Vertically transmitted – Horisontally received polarisation
VV	Vertically transmitted – Vertically received polarisation

## About FFI

The Norwegian Defence Research Establishment (FFI) was founded 11th of April 1946. It is organised as an administrative agency subordinate to the Ministry of Defence.

### FFI's MISSION

FFI is the prime institution responsible for defence related research in Norway. Its principal mission is to carry out research and development to meet the requirements of the Armed Forces. FFI has the role of chief adviser to the political and military leadership. In particular, the institute shall focus on aspects of the development in science and technology that can influence our security policy or defence planning.

### FFI's VISION

FFI turns knowledge and ideas into an efficient defence.

### FFI's CHARACTERISTICS

Creative, daring, broad-minded and responsible.

## Om FFI

Forsvarets forskningsinstitutt ble etablert 11. april 1946. Instituttet er organisert som et forvaltningsorgan med særskilte fullmakter underlagt Forsvarsdepartementet.

### FFIs FORMÅL

Forsvarets forskningsinstitutt er Forsvarets sentrale forskningsinstitusjon og har som formål å drive forskning og utvikling for Forsvarets behov. Videre er FFI rådgiver overfor Forsvarets strategiske ledelse. Spesielt skal instituttet følge opp trekk ved vitenskapelig og militærteknisk utvikling som kan påvirke forutsetningene for sikkerhetspolitikken eller forsvarsplanleggingen.

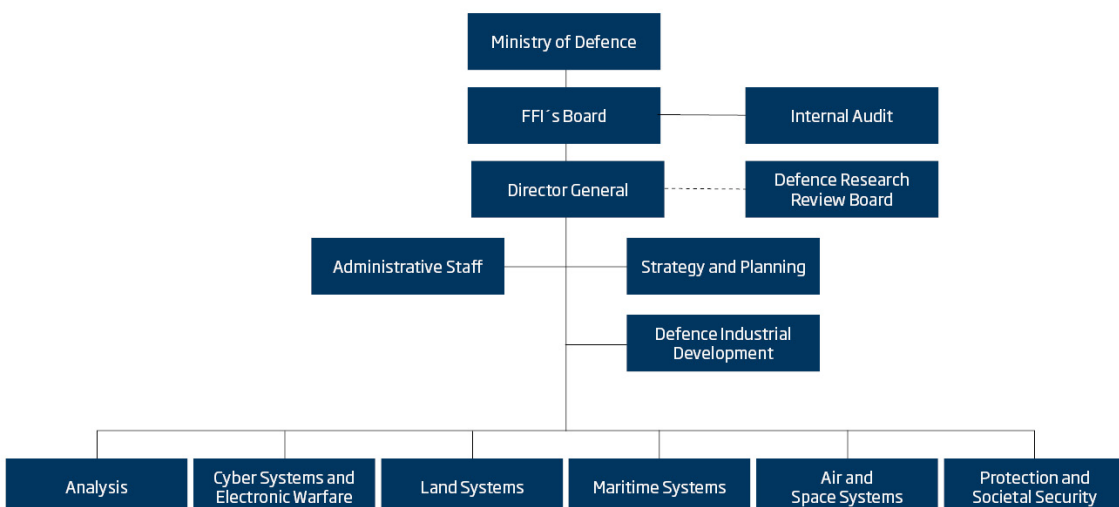
### FFIs VISJON

FFI gjør kunnskap og ideer til et effektivt forsvar.

### FFIs VERDIER

Skapende, drivende, vidsynt og ansvarlig.

## FFI's organisation





**Forsvarets forskningsinstitutt**  
Postboks 25  
2027 Kjeller

Besøksadresse:  
Instituttveien 20  
2007 Kjeller

Telefon: 63 80 70 00  
Telefaks: 63 80 71 15  
Epost: [ffi@ffi.no](mailto:ffi@ffi.no)

**Norwegian Defence Research Establishment (FFI)**  
P.O. Box 25  
NO-2027 Kjeller

Office address:  
Instituttveien 20  
N-2007 Kjeller

Telephone: +47 63 80 70 00  
Telefax: +47 63 80 71 15  
Email: [ffi@ffi.no](mailto:ffi@ffi.no)